

Stratifying Tropical Fires by Land Cover: Insights into Amazonian Fires, Aerosol Loading, and Regional Deforestation

J. E. Ten Hoeve¹, L. A. Remer², and M. Z. Jacobson¹

[1]{Department of Civil and Environmental Engineering, 473 Via Ortega, MC: 4020, Stanford University, Stanford, 94305, USA}

[2]{NASA/GSFC/Laboratory for Atmospheres, Greenbelt, MD, 20771, USA}

Abstract

This study analyzes changes in the number of fires detected on forest, grass, and transition lands during the 2002-2009 biomass burning seasons using fire detection data and co-located land cover classifications from the Moderate Resolution Imaging Spectroradiometer (MODIS). We find that the total number of detected fires correlates well with MODIS mean aerosol optical depth (AOD) from year to year, in accord with other studies. However, we also show that the ratio of forest to savanna fires varies substantially from year to year. Forest fires have trended downward, on average, since the beginning of 2006 despite a modest increase in 2007. Our study suggests that high particulate matter loading detected in 2007 was likely due to a large number of savanna/agricultural fires that year. Finally, we illustrate that the correlation between annual Brazilian deforestation estimates and MODIS fires is considerably higher when fires are stratified by MODIS-derived land cover classifications.

1. Introduction

Biomass burning is a large source of particulate matter over South America during the dry season [Artaxo *et al.*, 1998; Andreae *et al.*, 2002]. In addition to causing health problems,

1 particles also perturb the radiative balance, affect plant canopies, and modify cloud properties
2 [e.g., *Andreae et al.*, 2004]. In the tropics, fires are set to clear forests so that agricultural or
3 pastoral lands may be developed, but they are also set on existing agricultural or pastoral
4 lands for nutrient mobilization, pest control, and removal of brush and litter accumulation
5 [*Crutzen and Andreae*, 1990]. A number of studies to date have analyzed fire counts and fire
6 characteristics over the Amazon [*Setzer and Pereira*, 1991; *Kaufman et al.*, 1994; *Koren et*
7 *al.*, 2007, 2009; *Torres et al.*, 2010], and some have analyzed fire counts over different land
8 cover types [*Eva and Lambin*, 2000; *Eva and Fritz*, 2003; *Schroeder et al.*, 2005; *Morton et*
9 *al.*, 2008]. Our study differs from previous studies in that moderate-resolution land cover data
10 from across the entire Amazon basin are utilized to stratify fires by land cover, for all years
11 between 2002 and 2009. Our study also compares satellite measurements of fires with aerosol
12 loading, and attributes the source of the aerosol loading to forest and savanna fires
13 interannually.

14 Studies have found higher correlations between fires and deforestation if land cover
15 information is employed [*Eva and Fritz*, 2003]. Forest fires may be used as an indicator of
16 deforestation in the Amazon [*Setzer and Pereira*, 1991; *Eva and Fritz*, 2003], although these
17 fires are directly associated with some causes of deforestation (i.e. clear-cutting) and not
18 others (i.e. selective logging). Selective logging, which can increase a forest's flammability,
19 may lead to fires that are associated not with deforestation, but rather with forest degradation
20 [*Cochrane and Laurance*, 2002; *Fearnside*, 2005; *Asner et al.*, 2006]. However, since the
21 majority of Amazonian deforestation is attributed to land clearing for cattle ranching or
22 agriculture and forest fires are routinely associated with these types of deforestation, a
23 relationship between forest fires and deforestation is likely to be observed [*Setzer and*
24 *Pereira*, 1991; *Morton et al.*, 2006; *Morton et al.*, 2008].

1

2 **2. Data and Methods**

3 This study explores trends in detected MODIS fires between 2002 and 2009 over the Amazon,
4 during the biomass burning months of June through November. The region of interest
5 extends from coast to coast, between 0° and 20° S latitude and between 82° W and 34° W
6 longitude. The relatively high temporal and spatial resolution of the MODIS sensor, along
7 with predominantly clear or partially cloudy skies due to persistent high pressure during the
8 South American dry season, allows for daily detection of fires and aerosols [*Giglio et al.*,
9 2003; *Levy et al.*, 2007].

10 Daily 1-km Collection 5 Level 3 MODIS fire detections (MOD14A1) from the Terra
11 satellite are employed in the analysis [*Giglio et al.*, 2003; *Giglio et al.*, 2006], accessed from
12 The Land Processes Distributed Active Archive Center (<http://lpdaac.usgs.gov>). The morning
13 Terra overpass is used instead of the afternoon Aqua overpass because convective clouds are
14 less developed in the morning. Fires with a detection confidence lower than “high” (80%) are
15 excluded from the analysis due to possible false detections in small forest clearings [*Morton et*
16 *al.*, 2008; *Schroeder et al.*, 2008]. Fire detections are stratified into three land cover
17 categories: (1) forest, (2) savanna, and (3) transition between forest and savanna, according to
18 MODIS-derived land cover categories from the previous year. The Land Processes
19 Distributed Active Archive Center provides a combined Terra/Aqua yearly land cover product
20 (MCD12Q1). This product uses decision tree classification algorithms and training data to
21 assign land cover categories at 500-m resolution [*Friedl et al.*, 2010]. A majority filter is
22 applied to the 500-m land cover data to upscale the data to the 1-km fire product resolution.
23 The savanna category contains shrubland, savanna, grassland, cropland, and sparsely

1 vegetated and barren land. The transition land cover category is defined as 1-km² pixels that
2 do not have a majority land cover (i.e. 50% split between land cover categories).

3 Trends in aerosol loading are computed using the MODIS Collection 5 Level 3 aerosol
4 optical depth (AOD) at 550 nm [Levy *et al.*, 2007]. The monthly mean AOD product from the
5 Terra satellite (MOD08_M3) is employed to calculate a spatially- and temporally-averaged
6 AOD over our study region during the biomass burning season. Aerosol data is accessed from
7 the Level 1 and Atmosphere Archive and Distribution System
8 (<http://ladsweb.nascom.nasa.gov/>).

9 To compare yearly Brazilian fires detected by MODIS to measured Brazilian
10 deforestation rates, deforestation estimates from the Brazilian Instituto Nacional de Pesquisas
11 Espaciais (INPE) are employed (unpublished data, 2006;
12 <http://www.inpe.br/noticias/arquivos/pdf/prodes2009tabela1.pdf>). These estimates are
13 computed using the high-resolution Landsat sensor, as well as other satellites such as the
14 China-Brazil Earth Resources Satellite (CBERS), particularly when cloud cover is present.

16 3. Results

17 Figure 1 shows the interannual trend in daily MODIS fires, summed over all days between
18 June and November, in our study region between 2002 and 2009. Also plotted is the
19 interannual trend in average monthly AOD. Previous studies have shown a similar correlation
20 using AVHRR fires and MODIS AOD [Koren *et al.*, 2007], as well as MODIS fires and OMI
21 AOD [Torres *et al.*, 2010]. A Student's two-tailed t-test indicates that total fires and seasonal-
22 regional mean AOD are correlated at the 99% confidence level, with a correlation coefficient
23 of 96%. The high correlation suggests that the majority of the aerosol loading is due to

1 biomass burning fires, and not other sources such as dust or transported aerosol [*Koren et al.*,
2 2007]. A map of fire locations for each year is depicted in Figure S1 in the auxiliary material.

3 The sharp decrease in both fires and aerosol loading in 2006 has, in some studies, been
4 attributed to a tri-national alert service for wildfires enacted in 2006 in the wake of the severe
5 2005 drought [*Koren et al.*, 2007, 2009]. Other studies attribute this decline largely to
6 positive precipitation anomalies that year [*Schroeder et al.*, 2009; *Torres et al.*, 2010]. Figure
7 1 indicates that a high burning year followed in 2007, suggesting that the tri-national alert
8 service may not have been the cause of the 2006 decline. Figure 1 shows the basin-wide
9 interannual variability of fires and smoke, but it cannot explain the increase or decrease in
10 forest or savanna burning in particular. For that, land cover stratification must be applied.

11 Figure 2a illustrates yearly fire detections stratified by land cover category. Also
12 plotted is the ratio of forest fires to savanna fires each year. Within our study region, more
13 total savanna fires are detected than are forest fires or transition fires for each year. Thus, it is
14 probable that a significant portion of the aerosol loading in our study region is due to savanna
15 fires, in addition to forest fires. Forest fires generally exhibit a higher particulate matter
16 emission factor than savanna fires [*Janhäll et al.*, 2010], and also contain more biomass per
17 area than savanna or other land use types that fall within our “savanna” category, yet
18 combustion efficiencies are often lower [*Ward et al.*, 1992]. If forests were contributing the
19 bulk of particulate matter each year, we would expect the correlation between forest fires
20 alone and AOD to be equal to or higher than the correlation between total fires and AOD,
21 which it is not. The correlation between forest fires and AOD is 0.87 and the correlation
22 between savanna fires and AOD is 0.85. Both correlations are lower than the correlation
23 between total fires and AOD, 0.96, suggesting that savanna fires contribute appreciably to
24 aerosol loading in the region.

1 Figure 2a depicts a general decreasing trend in forest fires between 2006 and 2009.
2 Forest fire detections were only 30% higher in 2007 than in 2006, yet savanna fires were
3 300% higher in 2007 than in 2006. As a result, the 2007 peak in aerosol loading observed in
4 Figure 1 is likely due to an anomalously high number of savanna fire detections that year.
5 Large negative precipitation anomalies occurring over the southeastern Amazon and Cerrado
6 regions in 2007 match the location of anomalously high numbers of savanna fires that year
7 (auxiliary Figure S1, Figure S2) [*Janowiak and Xie*, 1999; *Morton et al.*, 2008; *Torres et al.*,
8 2010]. Similarly large negative precipitation anomalies occurred in 2005 (Figure S2), along
9 with a similarly high peak in AOD (Figure 1), yet the ratio of forest to savanna fires was over
10 twice as large in 2005 than in 2007, indicating an inherent difference in the type of burning
11 which occurred during these two years. Figure S2 indicates that the drought was more severe
12 and more extensive in 2005 than 2007, which may partly account for the difference in the
13 forest fire to savanna fire ratio between the two years.

14 Over the eight year data set, the highest forest fire to savanna fire ratio occurred in
15 2004 (0.62) and the lowest ratio occurred in 2008 (0.24). In 2008, forest and savanna fires
16 declined by nearly 60% compared to 2007, and declined another 50% between 2008 and
17 2009. This large decrease in both forest and savanna fire detections resulted in the lower
18 aerosol loadings observed in 2008 and 2009 (Figure 1). This decline may have resulted from
19 a combination of moderately positive precipitation anomalies, particularly in 2009, as well as
20 stricter fire regulations and/or a declining economy; however, it is difficult to conclusively
21 determine the cause of the reduction [*Torres et al.*, 2010].

22 Figure 2b shows fires stratified by land cover category, normalized by the area of each
23 land cover category. On average between 2002 and 2009, there were 5,226,760 km² of forest,
24 5,154,306 km² of savanna, and 305,025 km² of transition land in our study region. For each

1 year, the number of fires over transition land per square kilometer exceeded that over both
2 forest and savanna. This result agrees with previous studies of deforestation in the Amazon –
3 a large fraction of the land clearing and consequential burning occurs on the edge of the forest
4 frontier [Skole and Tucker, 1993; Cochrane, 2003]. Increased flammability along forest
5 edges may also play a role [Cochrane and Laurance, 2002]. Between 2002 and 2009, one fire
6 was detected for every 173 km² of forest, 71 km² of savanna, and 47 km² of transition land.

7 The methodology of stratifying fires by land cover type also results in higher
8 correlations between fire detections and deforestation. Figure 3 shows scatter plots and linear
9 least-squares regressions between MODIS fires summed over each biomass burning season
10 and INPE estimated deforestation for the country of Brazil. The correlation between total
11 fires and INPE deforestation is relatively low, 0.30 (Figure 3a). However, when only forest
12 fires are retained, the correlation is much higher, 0.65, which is significant at the 90%
13 confidence level (Figure 3b).

14 The middle and bottom row of panels in Figure 3 represent the number of fires
15 occurring on two-or-more and three-or-more days within each 1-km² pixel, respectively, for
16 each biomass burning season. These higher frequency fires are likely to be associated with
17 deforestation, as deforested wood is often piled and reburned on several occasions following
18 the initial burn [Morton *et al.*, 2008]. The stratified correlations in Figures 3e and 3f, 0.77 and
19 0.76, are significant at the 97% confidence level. Yet, the difference between the stratified
20 and non-stratified correlations in this second row is less than between Figure 3a and Figure
21 3b/c.

22 The bottom row of panels in Figure 3, which represents three-or-more fire detections
23 per pixel, shows nearly no difference in the correlation coefficients between the stratified and
24 non-stratified cases, yet correlations in all panels are significant at the 99% level.

1 Stratification improves the correlation to a lesser extent in the case of persistent fires because
2 persistent fires are often classified as forest or transition fires. Summed fires between 2002
3 and 2009 indicate that 53% (65%) of two-detection (three-detection) persistent fires occur on
4 forest or transition lands, compared with 33% of all fires. This method of correlating fires to
5 deforestation performs well in areas with high rates of clear-cutting deforestation, such as the
6 states of Mato Grosso or Pará [Fearnside, 2005; Morton *et al.*, 2006]. One should take
7 caution extending this methodology to other regions where deforestation and biomass burning
8 are not as closely linked, and where humid conditions prevent the widespread use of fires for
9 land management [Eva and Fritz, 2003].

11 **4. Conclusions**

12 This work demonstrates a statistically significant correlation between yearly MODIS AOD
13 and MODIS fire detections during the Amazon biomass burning seasons between 2002 and
14 2009. Stratifying fire detections by MODIS land cover type provides further information into
15 the source of the aerosol loading. A decreasing trend in forest fires is observed between 2006
16 and 2009, despite a modest increase in 2007. Results also indicate that high regional aerosol
17 loading detected in 2007 was likely caused by a high number of savanna/agricultural fires that
18 year, in part due to negative precipitation anomalies in the southeastern Amazon and Cerrado
19 regions. We also find that the number of fires occurring in transition regions, regions on the
20 edge of forest and savanna lands, is higher than both forest and savanna fires on a per area
21 land cover basis. Finally, we illustrate that the correlation between detected fires and annual
22 Brazilian deforestation estimates from high-resolution sensors becomes greater if fires are first
23 stratified by land cover type; however, when only persistent fires are employed, the

1 correlation does not improve with stratification since the majority of persistent fires occur
2 over forest and transition lands.

3 We acknowledge the various uncertainties associated with this analysis. A number of
4 fires may not be detected due to atmospheric conditions, satellite overpass time, or fire size
5 and energy. False fire detections may be included in the data, however, only high-confidence
6 fires were selected to minimize this error. Misclassified land cover data, especially near
7 regions of forest conversion, may also introduce potential uncertainty. Yet, this research
8 indicates that segregating fires by moderate-resolution land cover data provides a simple
9 method of gaining additional information about the source of regional aerosol loading and
10 about regional deforestation on interannual timescales.

12 **Acknowledgements**

13 This study was supported by NASA grant NNX07AN25G, the NASA Interdisciplinary
14 Sciences Program, and the NASA Earth Systems Science Fellowship. We thank Eric Lambin
15 for helpful comments.

17 **References**

18 Andreae, M. O., et al. (2002), Biogeochemical cycling of carbon, water, energy, trace gases,
19 and aerosols in Amazonia: The LBA-EUSTACH experiments, *J. Geophys. Res.*, *107*, D20,
20 8066, doi: 10.1029/2001JD000524.

21 Andreae, M. O., D. Rosenfeld, P. Artaxo, A. A. Costa, G. P. Frank, K. M. Longo, and M. A.
22 F. Silva-Dias (2004), Smoking rain clouds over the Amazon, *Science*, *303*(5662), 1337-1342.

1 Artaxo, P., E. T. Fernandes, J. V. Martins, M. A. Yamasoe, P. V. Hobbs., W. Maenhaut, K.
2 M. Longo, and A. Castanho (1998), Large-scale aerosol source apportionment in Amazonia,
3 *J. Geophys. Res.*, *103*, D24, doi: 10.1029/98JD02346.

4 Asner, G. P., E. N. Broadbent, P. J. C. Oliveira, M. Keller, D. E. Knapp, and J. N. M. Silva
5 (2006), Condition and fate of logged forests in the Brazilian Amazon, *Proc. Natl. Acad. Sci.*
6 *U. S. A.*, *103*(34), 12947-12950.

7 Cochrane, M. A. (2003), Fire science for rainforests, *Nature*, *421*, 913-919.

8 Cochrane, M. A., and W. F. Laurance (2002), Fires as a large-scale edge effect in Amazonian
9 forests, *J. Trop. Ecol.*, *18*(3), 311-325.

10 Crutzen, P. J., and M. O. Andreae (1990), Biomass burning in the tropics: Impact on
11 atmospheric chemistry and biogeochemical cycles, *Science*, *250*(4988), 1669-1678.

12 Eva, H., and E. F. Lambin (2000), Fires and land-cover change in the tropics: A remote
13 sensing analysis at the landscape scale, *J. Biogeogr.*, *27*(3), 765-776.

14 Eva, H. and S. Fritz (2003), Examining the potential of using remotely sensed fire data to
15 predict areas of rapid forest change in South America, *Appl. Geogr.*, *23*, 189-204.

16 Fearnside, P. M. (2005), Deforestation in Brazilian Amazonia: history, rates, and
17 consequences, *Conserv. Biol.*, *19*(3), 680-688.

18 Friedl, M. A., D. Sulla-Menashe, B. Tan, A. Schneider, N. Ramankutty, A. Sibley, and X.
19 Huang (2010), MODIS Collection 5 global land cover: Algorithm refinements and
20 characterization of new datasets, *Remote Sens. Environ.*, *114*, 168-182.

21 Giglio, L., I. Csiszar, and C. O. Justice (2006), Global distribution and seasonality of active
22 fires as observed with the Terra and Aqua Moderate Resolution Imaging Spectroradiometer
23 (MODIS) sensors, *J. Geophys. Res.*, *111*, G02016, doi: 10.1029/2005JG000142.

1 Giglio, L., J. Descloitres, C. O. Justice, and Y. J. Kaufman (2003), An enhanced contextual
2 fire detection algorithm for MODIS, *Remote Sens. Environ.*, *87*, 273-282.

3 Janhäll, S., M. O. Andreae, and U. Pöschl (2010), Biomass burning aerosol emissions from
4 vegetation fires: particle number and mass emission factors and size distributions, *Atmos.*
5 *Chem. Phys.*, *10*, 1427-1439.

6 Janowiak, J. E. and P. Xie (1999), CAMS-OPI: A global satellite-rain gauge merged product
7 for real-time precipitation monitoring applications, *J. Climate*, *12*, 3335-3342.

8 Kaufman, Y. J., B. N. Holben, D. Tanré, and D. E. Ward (1994), Remote Sensing of Biomass
9 Burning in the Amazon, *Remote Sensing Reviews*, *10*(1-3), 51 – 90.

10 Koren, I., L. A. Remer, and K. Longo (2007), Reversal of trend of biomass burning in the
11 Amazon, *Geophys. Res. Lett.*, *24*, L20404, doi: 10.1029/2007GL031530.

12 Koren, I., L. A. Remer, K. Longo, F. Brown, and R. Lindsey (2009), Reply to comment by W.
13 Schroeder et al. on “Reversal of trend of biomass burning in the Amazon”, *Geophys. Res.*
14 *Lett.*, *36*, L03807, doi: 10.1029/2009GL036063.

15 Levy, R. C., L. A. Remer, S. Mattoo, E. F. Vermote, and Y. J. Kaufman (2007), Second-
16 generation operational algorithm: Retrieval of aerosol properties over land from inversion of
17 Moderate Resolution Imaging Spectroradiometer spectral reflectance, *J. Geophys. Res.*, *112*,
18 D13211, doi:10.1029/2006JD007811.

19 Morton, D. C., R. S. DeFries, J. T. Randerson, L. Giglio, W. Schroeder, and G. R. van der
20 Werf (2008), Agricultural intensification increases deforestation fire activity in Amazonia,
21 *Glob. Change Biol.*, *14*, 2262-2275.

22 Morton, D. C., R. S. DeFries, Y. E. Shimabukuro, L. O. Anderson, E. Arai, F. del bon
23 Espirito-Santo, R. Freitas, and J. Morissette (2006), Cropland expansion changes deforestation

1 dynamics in the southern Brazilian Amazon, *Proc. Natl. Acad. Sci. U. S. A.*, 103(39), 14637-
2 14641.

3 Schroeder, W., L. Giglio, and J. A. Aravéquia (2009), Comment on “Reversal of trend of
4 biomass burning in the Amazon” by Ilan Koren, Lorraine A. Remer, and Karla Longo,
5 *Geophys. Res. Lett.*, 36, L03806, doi: 10.1029/2008GL035659.

6 Schroeder, W., J. Morisette, I. Csiszar, L. Giglio, D. Morton, and C. O. Justice (2005),
7 Characterizing vegetation fire dynamics in Brazil through multi-satellite data: Common trends
8 and practical issues, *Earth Interact.*, 9, 1-26.

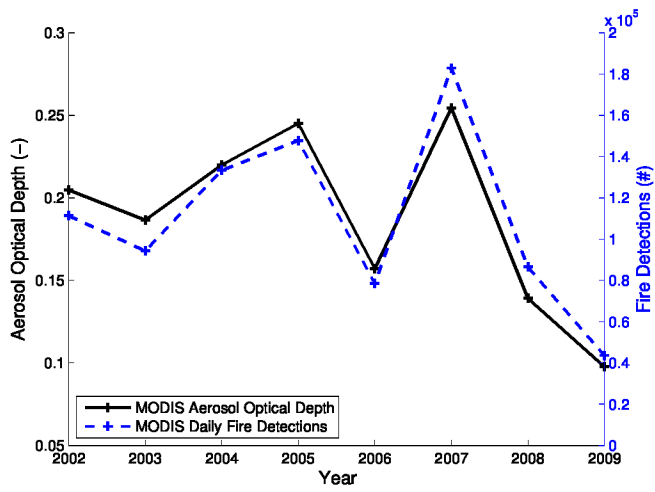
9 Schroeder, W., E. Prins, L. Giglio, I. Csiszar, C. Schmidt, J. T. Morisette, and D. Morton
10 (2008), Validation of GOES and MODIS active fire detection products using ASTER and
11 ETM+ data, *Remote Sens. Environ.*, 111, 2711-2726.

12 Setzer, A. W., and M. C. P. Pereira (1991), Amazonia biomass burnings in 1987 and an
13 estimate of their tropospheric emissions, *Ambio*, 20, 19-22.

14 Skole, D. and C. Tucker (1993), Tropical deforestation and habitat fragmentation in the
15 Amazon: Satellite data from 1978 to 1988, *Science*, 260(5116), 1905-1910.

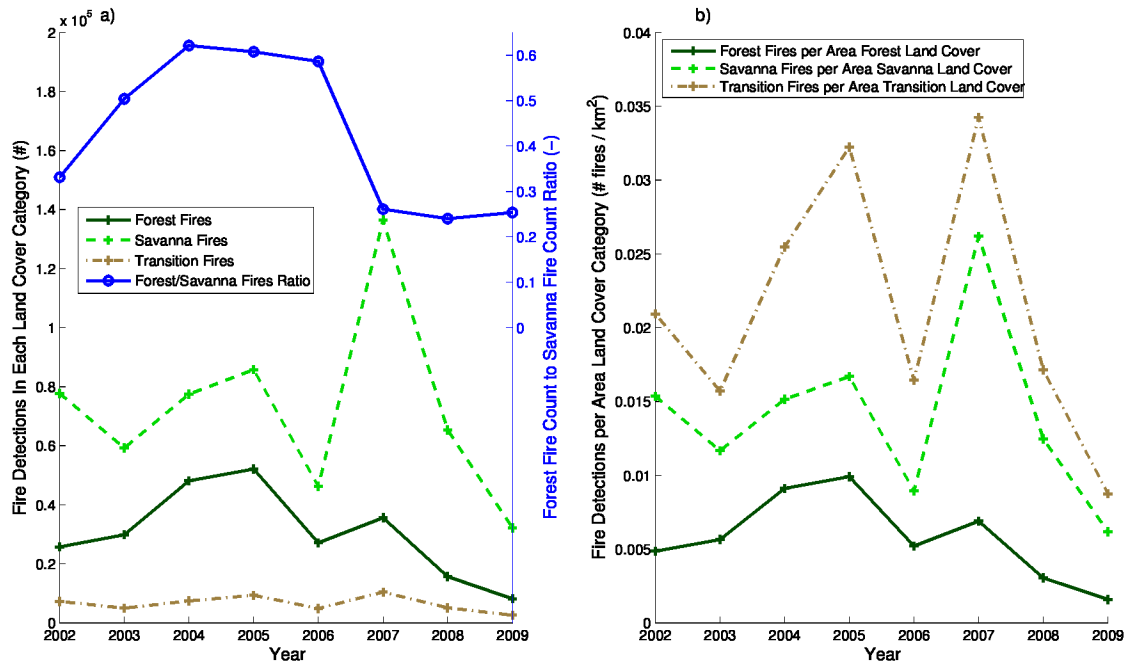
16 Torres, O., Z. Chen, H. Jethva, C. Ahn, S. R. Freitas, and P. K. Bhartia (2010), OMI and
17 MODIS observations of the anomalous 2008-2009 Southern Hemisphere biomass burning
18 seasons, *Atmos. Chem. Phys.*, 10, 2505-2513.

19 Ward, D. E., R. A. Susott, J. B. Kauffman, R. E. Babbitt, D. L. Cummings, B. Dias, B. N.
20 Holben, Y. J. Kaufman, R. A. Rasmussen, and A. W. Setzer (1992), Smoke and fire
21 characteristics for cerrado and deforestation burns in Brazil: BASE-B experiment, *J. Geophys.*
22 *Res.*, 97(D13), 14601-14619, doi:10.1029/92JD01218.



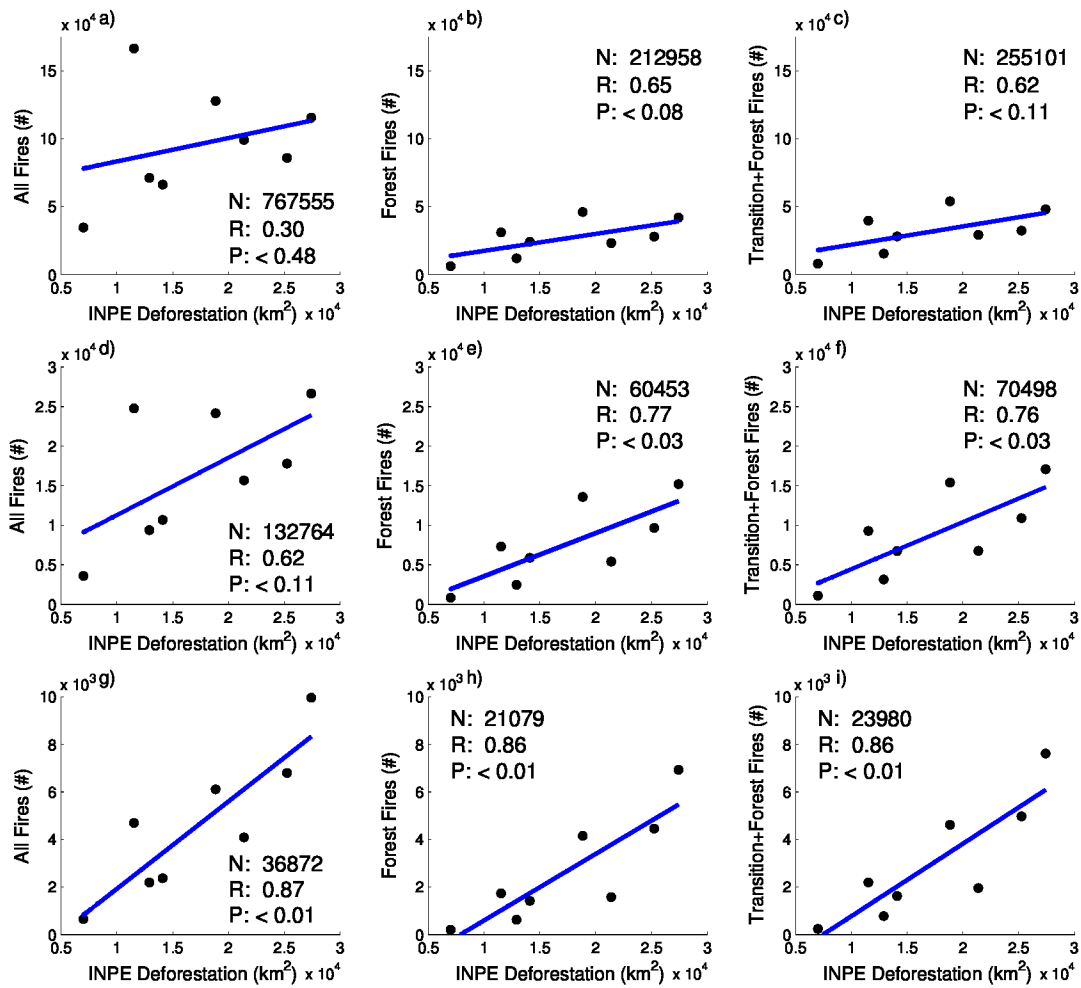
1

2 Figure 1: Interannual trend of seasonally-averaged MODIS Terra AOD and interannual trend
 3 in total MODIS Terra daily fire detections over the Amazon biomass burning season (Jun –
 4 Nov), for the years between 2002 and 2009.



1

2 Figure 2: (a) Interannual trend of MODIS fire detections during the Amazon biomass burning
3 season, stratified by MODIS land cover categories from the previous year, between 2002 and
4 2009. Also plotted is the ratio of forest fires to savanna fires for each year. (b) Interannual
5 trend of MODIS fire detections stratified by land cover category, per total area of each land
6 cover category in the study domain.



1

2 Figure 3: (a) Scatter plot and linear least-squares regression between MODIS detected fires
3 over Brazil and Instituto Nacional de Pesquisas Espaciais (INPE) Brazilian deforestation
4 estimates for the years between 2002 and 2009. (b) Same as (a) but only including fires over
5 the forest land cover category. (c) Same as (a) but only including fires over the forest and
6 transition land cover categories. (d)-(f) Scatter plots between two-day persistent fires, defined
7 as fires with two or more detections occurring over the same 1-km² pixel in a single biomass
8 burning season, and INPE deforestation. (g)-(i) Scatter plots between three-day persistent
9 fires, defined as fires with three or more detections occurring over the same 1-km² pixel, and
10 INPE deforestation. The summation of fires between 2002 and 2009 (N), the Pearson's
11 correlation (R), and the non-directional p-value (P) are also included in each panel.